AD-A260 969

1. AGENCY USE ONLY (Leave blank)	2. REPORT DATE	3. REPORT TYPE AND DATES COVERED
	December 21, 1992	Final March 31 - September 30, 1992

4. TITLE AND SUBTITLE
New Pyro-Optic Techniques for Imaging of Long Wavelength IR-Radiation (Pyro-Optic Initiation Program)

5. FUNDING NUMBERS
DAAL03-92-G-0036

6. AUTHOR(S)
L. E. Cross
A. S. Bhalla

7. PERFORMING ORGANIZATION NAME(S) AND ADDRESS(ES)
Materials Research Laboratory
The Pennsylvania State University
University Park, PA 16802-4800

8. PERFORMING ORGANIZATION REPORT NUMBER

9. SPONSORING / MONITORING AGENCY NAME(S) AND ADDRESS(ES)
U. S. Army Research Office
P. O. Box 12211
Research Triangle Park, NC 27709-2211

10. SPONSORING / MONITORING AGENCY REPORT NUMBER
ARO 28784.1-PH

11. SUPPLEMENTARY NOTES
The view, opinions and/or findings contained in this report are those of the author(s) and should not be construed as an official Department of the Army position, policy, or decision, unless so designated by other documentation.

12a. DISTRIBUTION / AVAILABILITY STATEMENT
Approved for public release; distribution unlimited.

12b. DISTRIBUTION CODE

13. ABSTRACT *(Maximum 200 words)*

From a simple consideration of the thermal conversation efficiency which can be realized in the non contact pyro-optic system it is shown that for f/1 optics a scene temperature change of 0.1°C will realize a change at the detector of 10^{-3}°C for a detector thickness of 0.1 μ meter, chopping frequency of 25 Hz.

For a simple pixel element 50μ × 50μ × 0.1μ the RMS thermal noise limit in SbSI is calculated to be $3.5 \cdot 10^{-5}$°C well below the expected signal level.

Using a very simple ellipsometric setup working into a photomultiplier detector it is shown that for SbSI single crystals and thin films, temperature oscillations of 10^{-3}°C can be detected above noise level.

14. SUBJECT TERMS	15. NUMBER OF PAGES
	20
	16. PRICE CODE

17. SECURITY CLASSIFICATION OF REPORT	18. SECURITY CLASSIFICATION OF THIS PAGE	19. SECURITY CLASSIFICATION OF ABSTRACT	20. LIMITATION OF ABSTRACT
UNCLASSIFIED	UNCLASSIFIED	UNCLASSIFIED	UL

MASTER COPY: PLEASE KEEP THIS "MEMORANDUM OF TRANSMITTAL" BLANK FOR REPRODUCTION PURPOSES. WHEN REPORTS GENERATE UNDER ARO SPONSORSHIP, FORWARD A COMPLETED COPY OF THIS FORM WITH EACH REPORT TO OUR OFFICE. THIS WILL ASSURE PROPER IDENTIFICATION.

MEMORANDUM OF TRANSMITTAL

U.S. Army Research Office
ATTN: SLCRO-IP-Library
P.O. Box 12211
Research Triangle Park, NC 27709-2211

Dear Library Technician:

☐ Reprint (15 copies) ☐ Technical Report (50 copies)

☐ Manuscript (1 copy) ☒ Final Report (50 copies)

☐ Thesis (1 copy)

☐ MS ☐ PhD ☐ Other_____

TITLE: New Pyro-Optic Techniques for Imaging of Long Wavelength IR-Radiation (Pyro-Optic Initiation Program)

is forwarded for your information.

SUBMITTED FOR PUBLICATION TO (applicable only if report is manuscript):

N/A

Sincerely,

Dr. L. Eric Cross

NEW PYRO-OPTIC TECHNIQUES FOR IMAGING OF LONG WAVELENGTH IR-RADIATION
(Pyro-Optic Initiation Program)

FINAL REPORT

L. E. CROSS and A. S. BHALLA

March 31, 1992 to September 30, 1992

U. S. ARMY RESEARCH OFFICE

GRANT #DAAL03-92-G-0036

MATERIALS RESEARCH LABORATORY
THE PENNSYLVANIA STATE UNIVERSITY
UNIVERSITY PARK, PA 16802-4800

I. INTRODUCTION

In any thermal detector system for long wavelength infrared radiation, there are two distinct and separable functions which control the sensitivity.

(a) The thermal conversion efficiency i.e. the manner in which the absorbing detector chip converts the chopped IR radiation field into a fluctuating temperature.

(b) The thermometric sensing function of the element which converts the generated temperature change into as readable electrical or optical signal.

This relationship is depicted in equation 1.

		(a)		(b)	
RESPONSIVITY	=	Induced Temperaturature Change at the element.	×	Thermometric sensitivity of the element.	(1)

Earlier detection systems have focused primarily upon the function (b), developing systems such as the pyroelectric detector which have quite exceptional thermometric conversion efficiency, but which lead inevitably in the associated interconnect systems to very poor thermal conversion efficiency.

In the pyro-optic system we focus on an interrogation system using visible light which needs to make no thermal contact with the sample. The detection element can be given radiation limited boundary conditions by mounting on a transparent aerogel substrate, so that the thermal capacity of the element can be greatly reduced. Since the temperature signal is now vastly enhanced, the lower thermometric efficiency of the reflective mode optical ellipsometric interrogation can be tolerated.

In this initial study, we calculate first the thermal conversion efficiency for a model detecting element of the size required for a single pixel in a long wavelength IR imager. The thermal mass is taken down to the level permitted by the very low thermal contact with the environment afforded by the mounting upon a critically dehydrated transparent aerogel substrate. For such a very low thermal mass element, the RMS thermal fluctuation noise will clearly be strongly enhanced, however it is shown that for the conditions chosen to optimize the pyrooptic system the noise signal is still two orders of magnitude below the expected signal level.

For the ellipsometric optical detection scheme it is very difficult to derive theoretically the limiting noise floor. Thus, the emphasis of the present study has been to demonstrate experimentally using a controlled AC temperature source, that the level of signal which will be achieved by the enhanced thermal conversion can be clearly discerned above the practical instrumental noise floor in the optical detection system, if the best pyroelectric crystal is used. We believe that this is a more stringent test of feasibility in view of the complexity of any possible theoretical derivation.

2. THERMAL CONSIDERATIONS

For a uniform thermal scene illuminating a minimally heat sunk detector element through a sinusoidal chopper working at a frequency ω focused by an objective lens of F number I. The time dependent power reading the detector is given by

$$P = \frac{I_o A}{2f^2} \cos wt \, \Delta T_s \tag{2}$$

ΔT_s is the difference in temperature between the scene and the chopper.

I_o is the scene contrast in f/I (for the full 8-14 μ band $I_o \sim 5.10^{-5}$ W/cm^2).

The temperature rise at the detector ΔT_d is given by

$$\Delta T_d = \frac{I_o \Delta T_s}{2f^2 \omega cd} \sin wt. \tag{3}$$

where d is the detector thickness and c the volume specific heat of the detector.

For a chopping frequency of 25Hz, a detector thickness of 0.1μ meters and a volume specific heat of 2.2 Joules/cm^3°C (as for SbSI) using f/1 optics

$$\frac{\Delta T_d}{\Delta T_s} \sim 1.5 \cdot 10^{-2}. \tag{4}$$

Thus to discriminate a 0.1°C change at the object plane, the imager must be capable of resolving a $1.5 \cdot 10^{-3}$°C temperature change at the detector chip.

For the very thin detector chip acting as a single pixel of a thermal imaging system one must worry that the ultra high thermal conversion efficiency will be accompanied with high RMS thermal noise.

Taking the simple expression for the uncorrelated temperature fluctuations$\theta\mu$

$$\theta\mu^2 = \frac{kT_a^2}{cbA} \tag{5}$$

where k is the Boltzmann constant.

T_a the detector element temperature (290°K).

c the volume specific heat.

A the element area.

For a pixel element 50 × 50 μ meters, 0.1 μ meter thick with C = 2.2. J/cm^3°C working at room temperature (290°K) the RMS θ_c is

$$\theta_c = 3.4 \cdot 10^{-5}\text{°C}. \quad (6)$$

Almost two full orders of magnitude below the temperature change generated in the detector at the 0.1°C change in the scene.

3. THERMOMETRIC SENSITIVITY

In our earlier studied bismuth vanadiate $BiVO_4$, molybdenum disulphate MoS_2 and antimony sulphur ioxide SbSI were chosen as candidate thermo-optic crystals and the sensitivity of the reflectance coefficient to a small AC temperature modulation was evaluated using null ellipsometry to chose the optimum optical interrogation wavelength (figures 1 and 2). SbSI was found in these studies to be the most sensitive material and all subsequent experiments have been performed on this material both in single crystal and in thin film forms.

In figure 2, the function generator supplies a low frequency AC signal to the power amplifier which drives the AC temperature change in the thermoelectric element. A DC bias was used to set the background temperature. The SbSI single crystals were cemented directly to the thermoelectric using a heat conductive cement.

The change in the reflectance coefficient with temperature was measured by converting the output current of the photomultiplier to voltage, and amplifying in an amplifier phase locked to the driving power amplifier signal. Results on the single crystal samples were as follows:

1. The maximum change in reflectance coefficient occurs for optical wavelengths in the range 580 to 633 nm at ~18.4°C(fig. 3).

2. There is a linear dependence of the 633 nm reflectance at 17.5°C as a function of the AC temperature (fig. 4).

3. For the signal at 0.02°C which was the minimum that could be read on the thermocouple, noise in the optical system was not detectable. Even for an increase of ×25 in the gain the noise was still much less than the optical signal, i.e. the signal to noise ratio at 0.02°C is better than 25:1.

4. The signal to noise ratio suggests that levels of 10^{-3}°C will be observable above noise as is required by the thermal calculations.

Recently this extrapolation has been confirmed by improving the photon detector, cooling the photomultiplier tube, and by improving the sensitivity of the thermocouple detector which monitors the thermoelectric temperature rise.

Figure 6 shows the extended linear range of the reflectance response in SbSI at 16.3°C, 633 nm and 3.2 Hz chopping frequency.

Figure 7 shows the reflectance response under a temperature modulation of 4.10^{-3}°C and Fig. 8 shows the noise level with the modulation set at 0°C. Clearly a signal to noise ratio of order 2 exists for 4.10^{-3}°C.

Figure 9 and Table I summarize these measurements together with earlier data taken on MoS_2 and $BiVO_4$ crystals.

To take the system closer to the requirements for the pyro-optic system we have made preliminary studies on thin films of SbSI deposited on several potential substrates including GaAs, mica and glass.

Figures 10-12 show the results for films on mica, and figures 13 and 14 show the results on glass and on GaAs respectively.

The overall summary for both single crystals and films is given in Table II. If we use the extrapolation to arrive at limiting sensitivity from figures 11 and 12 we expect that the films also will be able to read temperatures ~10^{-3}°C.

4. SUMMARY AND CONCLUSIONS

From a simple consideration of the thermal conversation efficiency which can be realized in the non contact pyro-optic system it is shown that for f/1 optics a scene temperature change of 0.1°C will realize a change at the detector of 10^{-3}°C for a detector thickness of 0.1 μ meter, chopping frequency of 25 Hz.

For a simple pixel element $50\mu \times 50\mu \times 0.1\mu$ the RMS thermal noise limit in SbSI is calculated to be $3.5 \cdot 10^{-5}$°C well below the expected signal level.

Using a very simple ellipsometric setup working into a photomultiplier detector it is shown that for SbSI single crystals and thin films, temperature oscillations of 10^{-3}°C can be detected above noise level. Clearly many additional steps are needed to realize first a point detector, then an IR imaging system. We believe however that under highly constrained budget conditions we have been able to accomplish three of the key steps towards this realization.

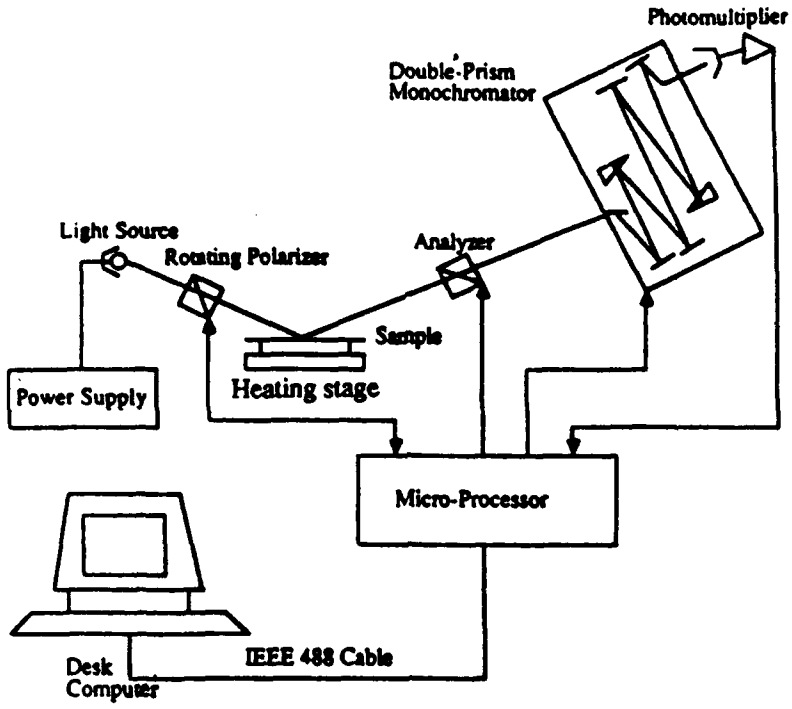

Figure 1. A schematic representation of automated spectroscopic ellipsometer

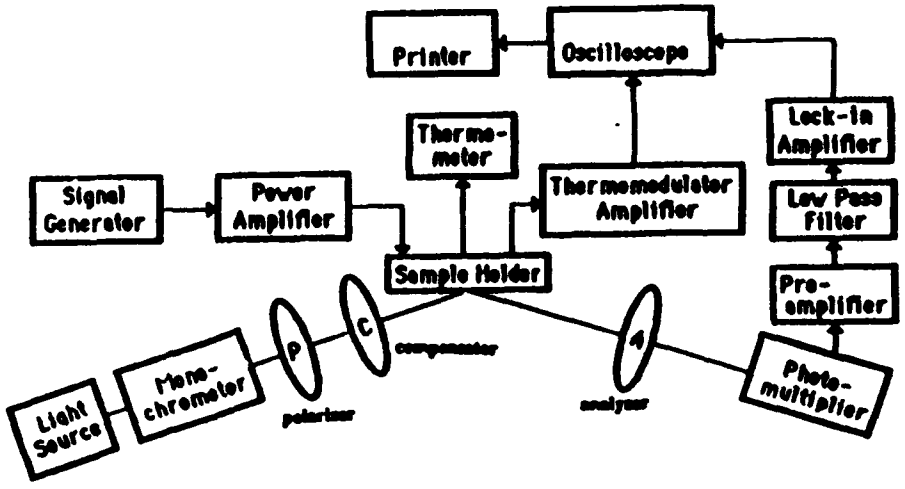

Figure 2. Schematic drawing of the exprimental equipment set up. P: polarizer, C: compensator, A: analyzer.

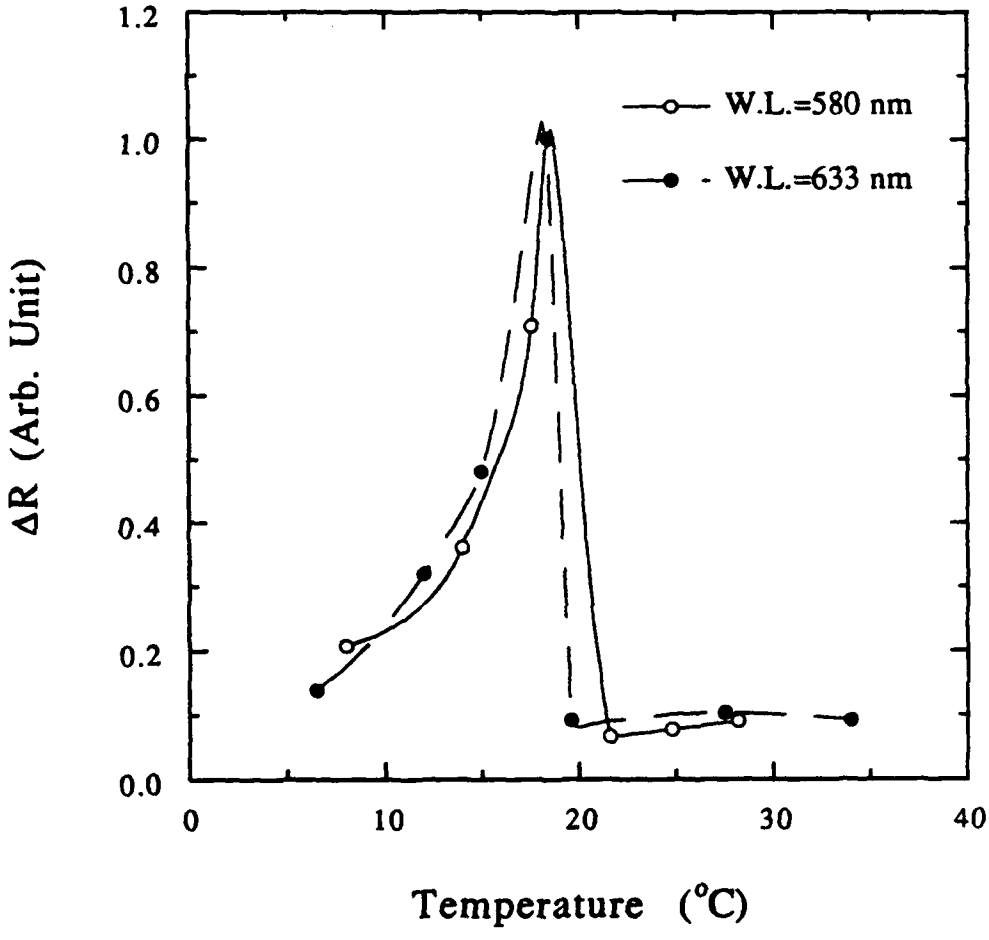

Figure 3 The change of the 633 and 580 nm reflectance coefficient of SbSI single crystal with temperature modulation. The base temperature was between 5 and 35°C with a 3.7 Hz AC modulation of approximately 0.02°C.

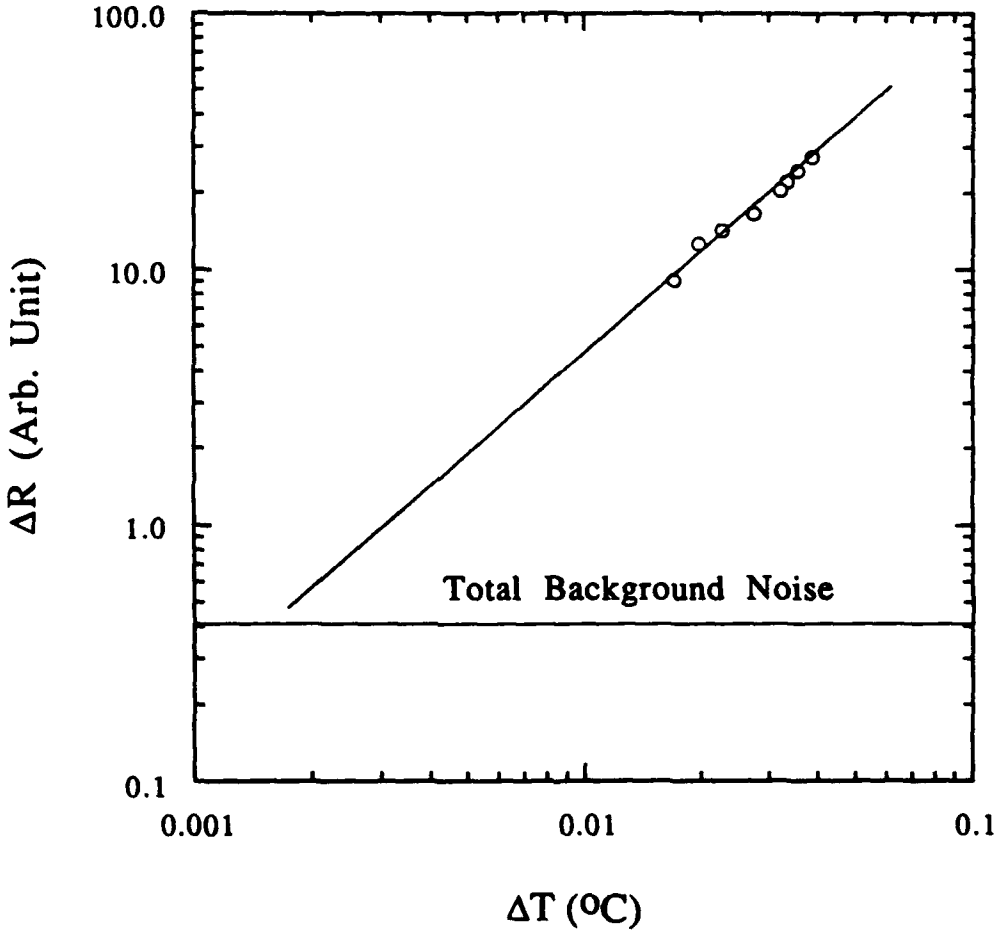

Figure 4 The dependence of the 633 nm reflectance coefficient of SbSI single crystal at 17.5°C on the magnitude of the temperature modulation. The frequency of the modulation was 3.7 Hz.

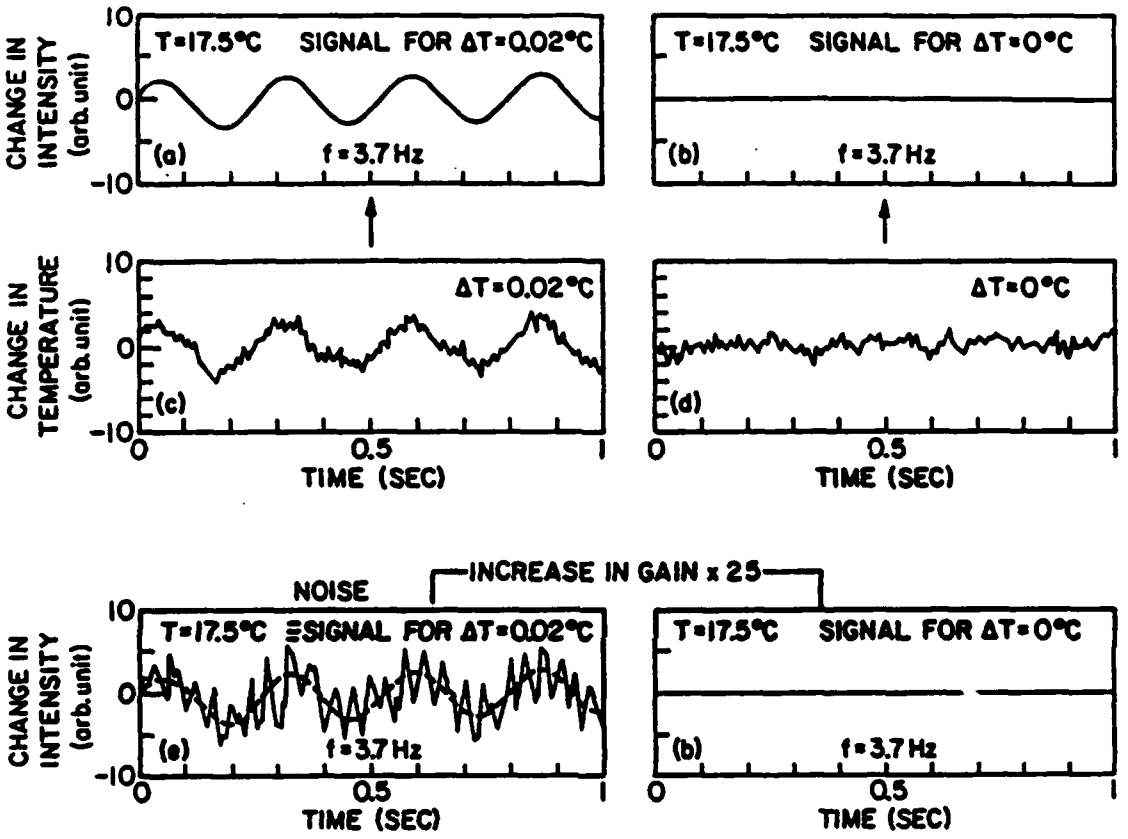

Figure 5 The temperature sensitivity of the reflectance coefficient to a small AC temperature modulation (ΔT) for SbSI single crystal. (a) The modulation of the reflectance coefficient, (b) the background noise in the reflectance modulation, (c) the temperature modulation ($\Delta T=0.02^{o}C$), (d) the background noise in the temperature modulation, (e) the background noise in the reflectance modulation (gain of the lockin amplifier increased by a factor of 25) with the modulation of the reflectance coefficient ($\Delta T=0.02^{o}C$) superimposed.

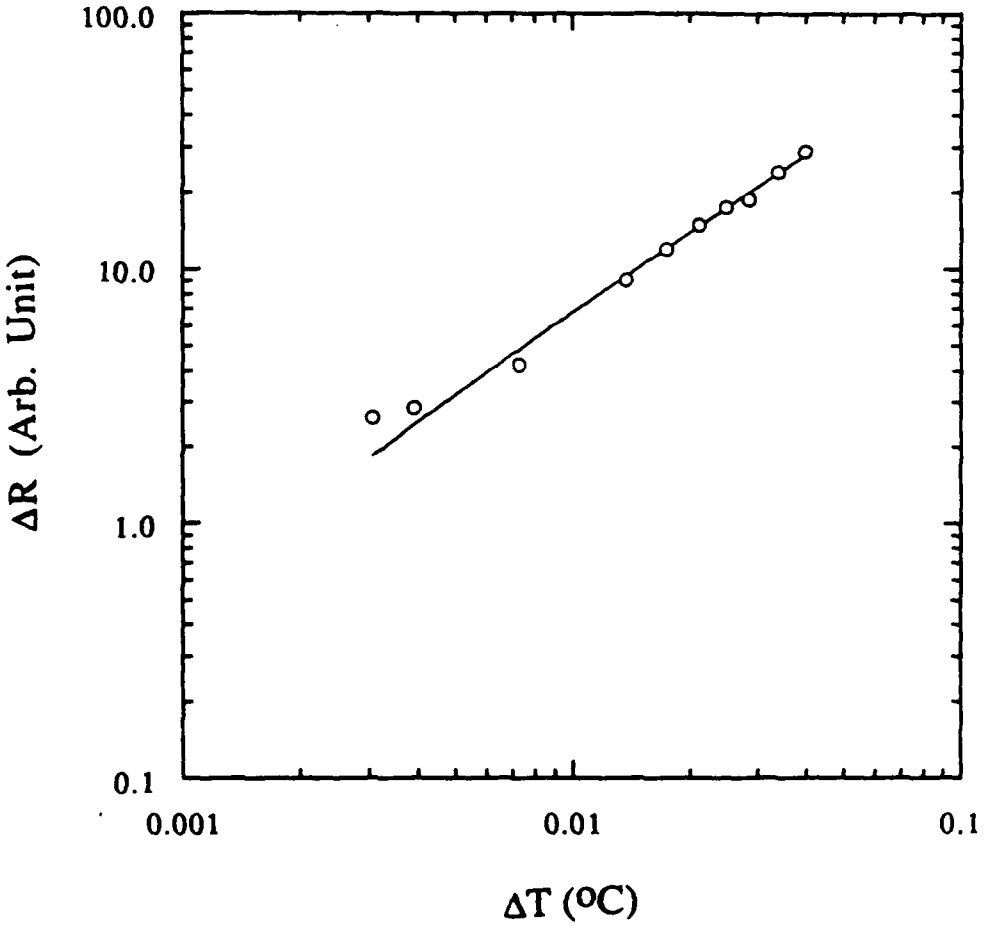

Figure 6 The dependence of the 633 nm reflectance coefficient of SbSI single crystal at 16.3°C on the magnitude of the temperature modulation. The frequency of the temperature modulation was 3.2 Hz. This data was taken after the improvement of the sensitivity of the system.

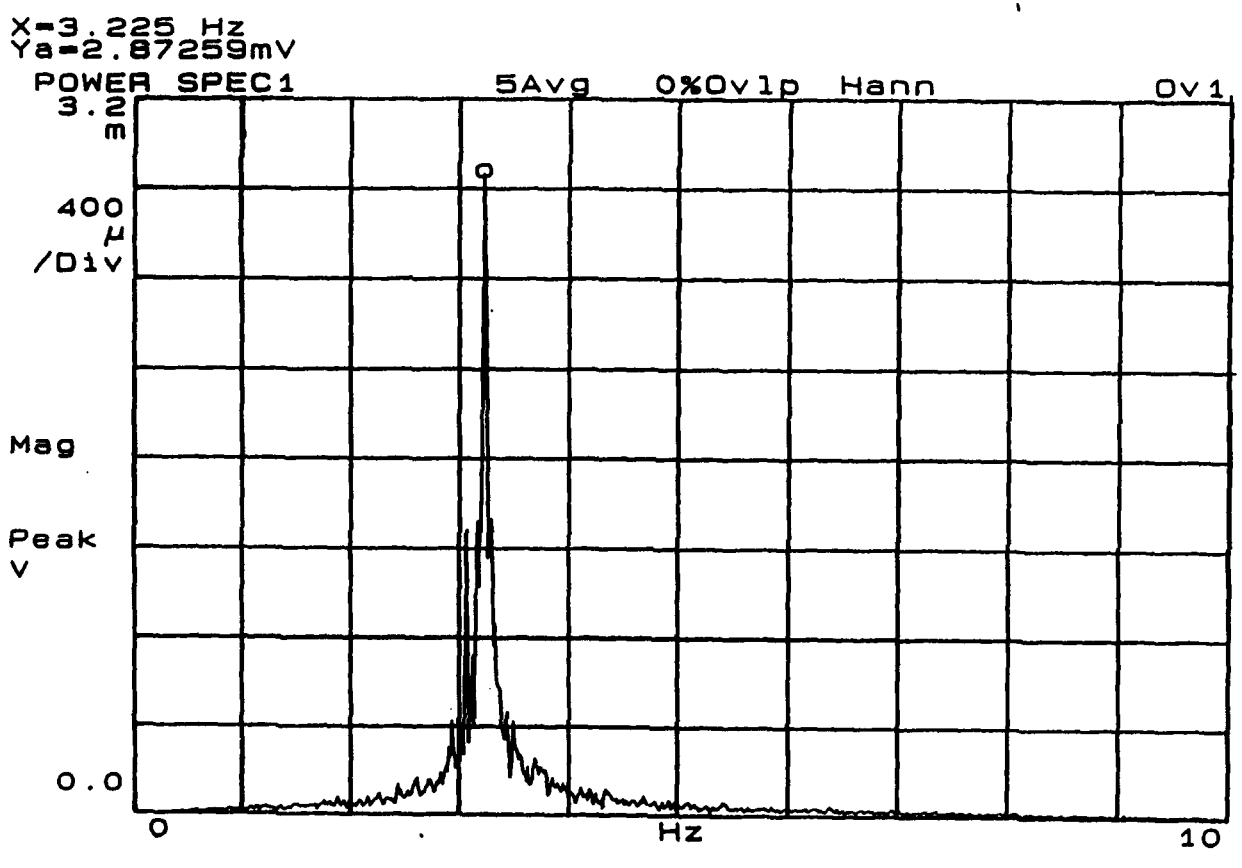

Figure 7 The signal of reflectance response of SbSI single crystal under a temperature modulation 4×10^{-3}°C

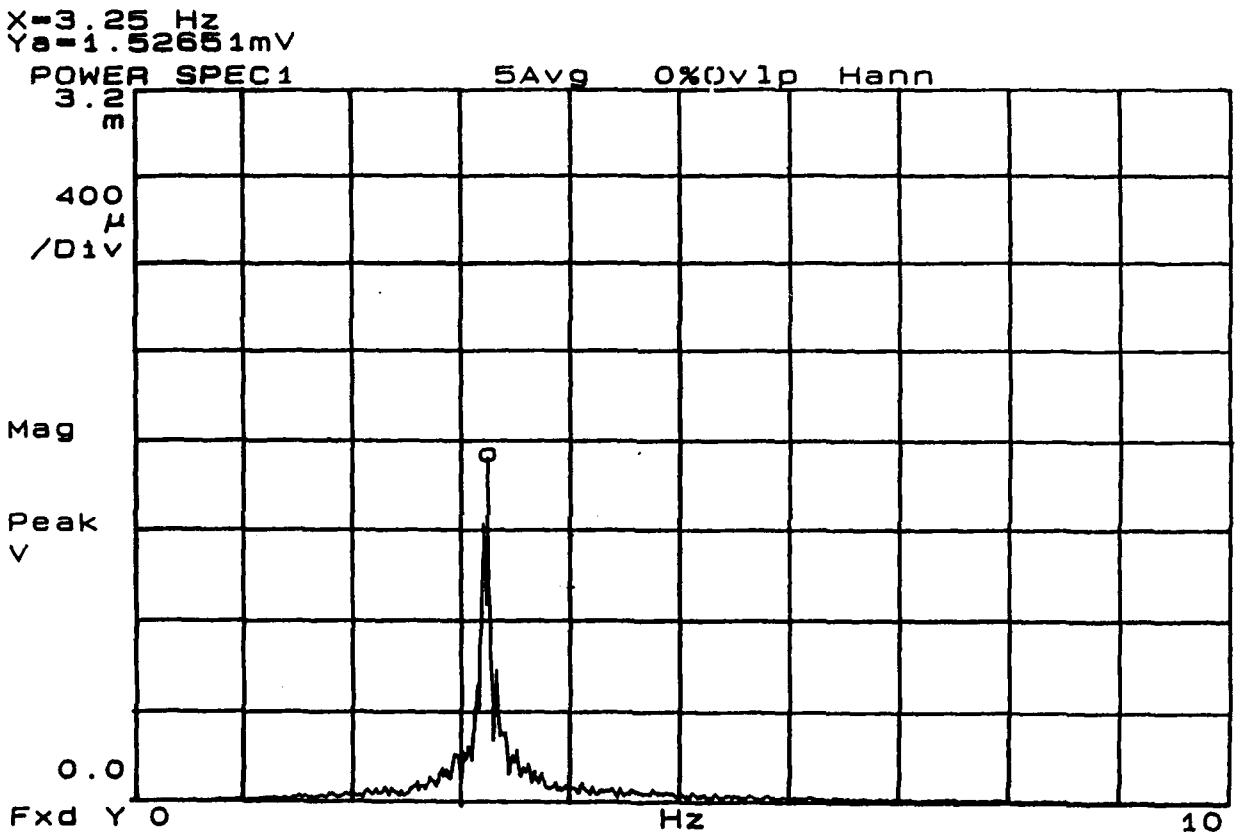

Figure 8 The noise level. This signal was obtained by setting the temperature modulation to zero.

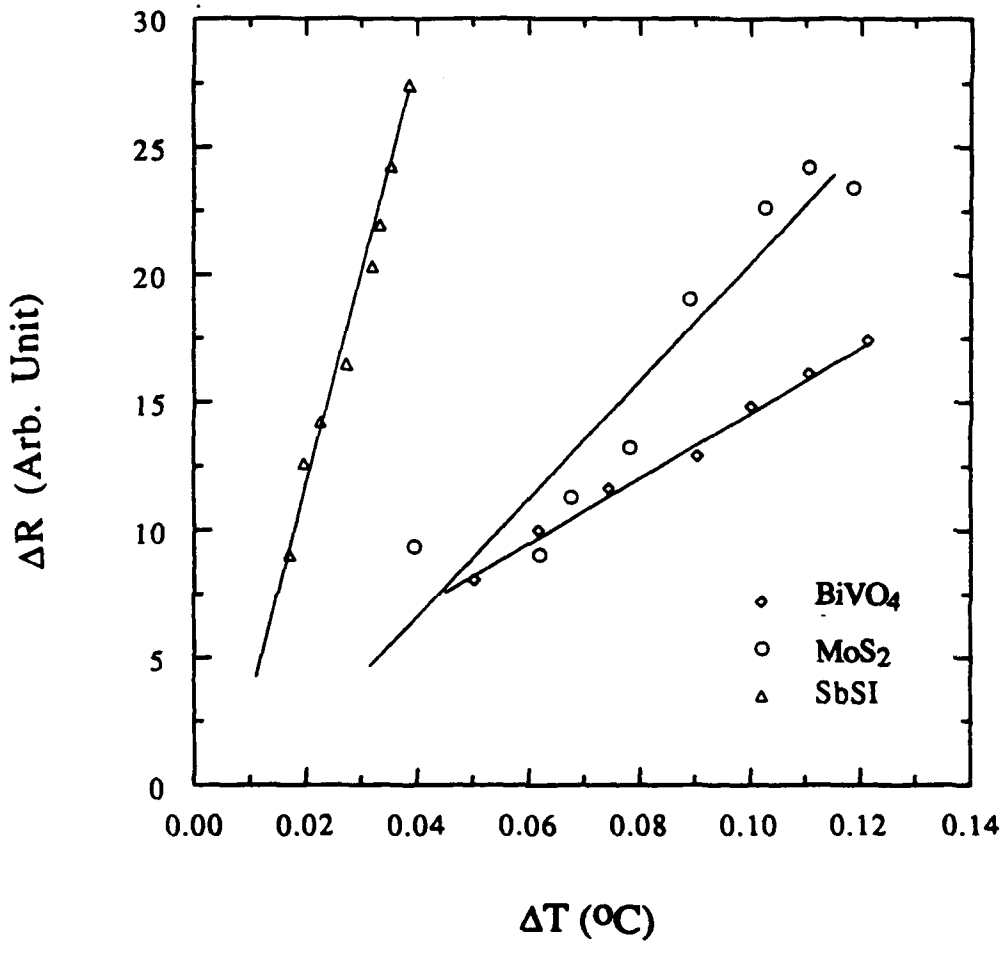

Figure 9 The relative dependence of the 633, 670 and 600 nm reflectance coefficients on the amplitude of the temperature modulation for SbSI, MoS_2 and $BiVO_4$, respectively.

Table 1 Summary of the experimental results where λ_{max} is the wavelength of maximum sensitivity, $\Delta\langle n\rangle/\Delta T$ is the temperature derivative of the refractive index and ΔT_{min} is the minimum temperature detected by monitoring the reflectance coefficient.

Material	λ_{max} (nm)	$\frac{\Delta\langle n\rangle}{\Delta T}(^{o}C^{-1})$	$\Delta T_{min}(^{o}C)$	Temperatuire Range (^{o}C)
SbSI	633	$7x10^{-2}$	10^{-3}	15 to 19
MoS_2	670	-10^{-2}	10^{-2}	-100 to 100
$BiVO_4$	600	$-2x10^{-3}$	10^{-2}	20 to 240

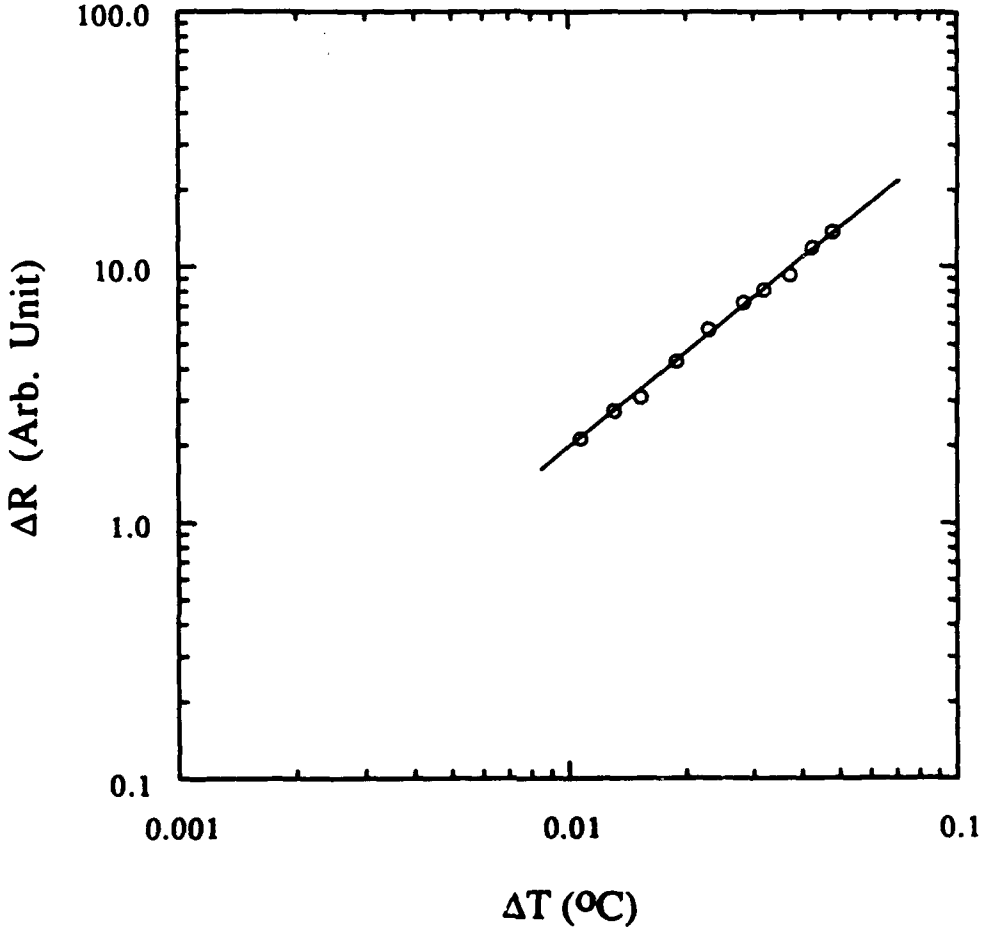

Figure 10 The reflectance coefficient response as a function of the magnitude of the temperature modulation for the SbSI film on a mica substrate. The base temperature was 19.5°C, the wavelength was 600 nm, and the frequency of the temperature modulation was 2.125 Hz.

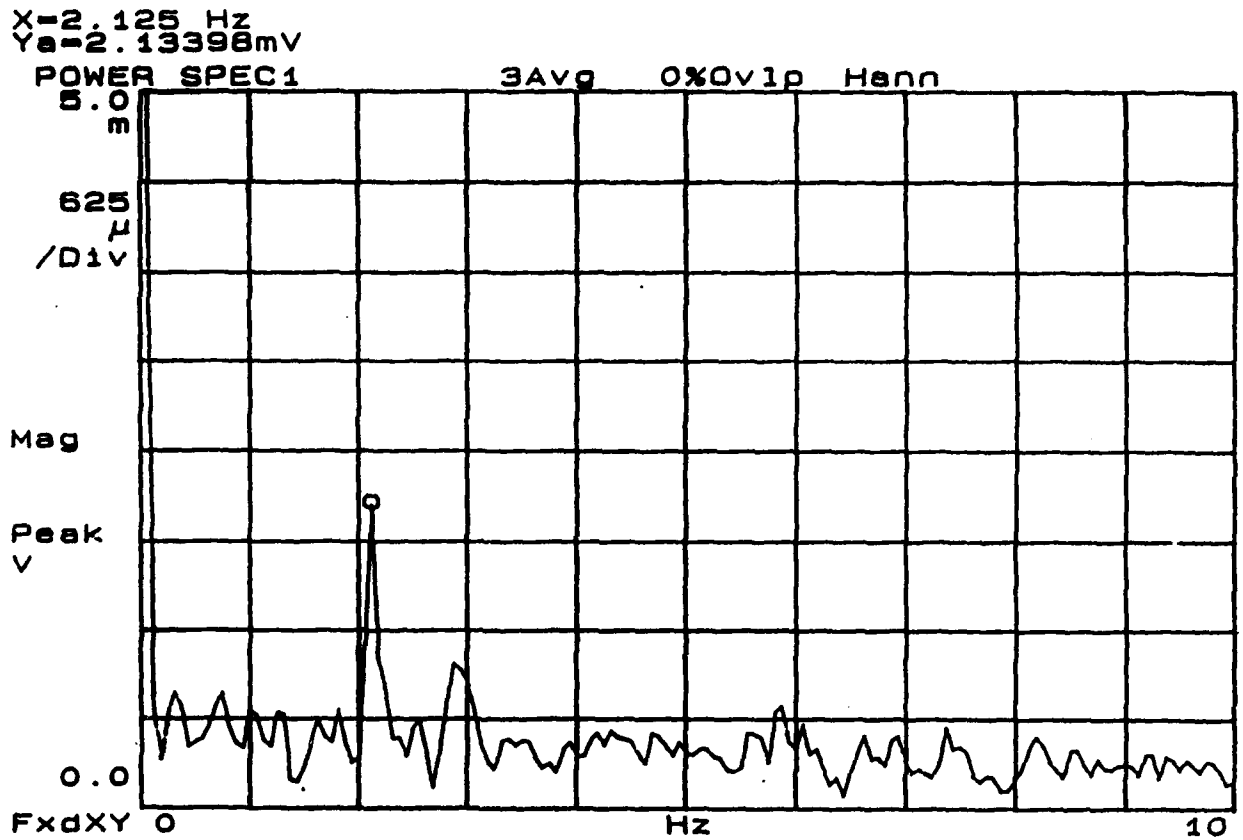

Figure 11 The signal of 600 nm reflectance modulation for a SbSI thin film on mica using a temperature modulation of 1.1×10^{-2}°C.

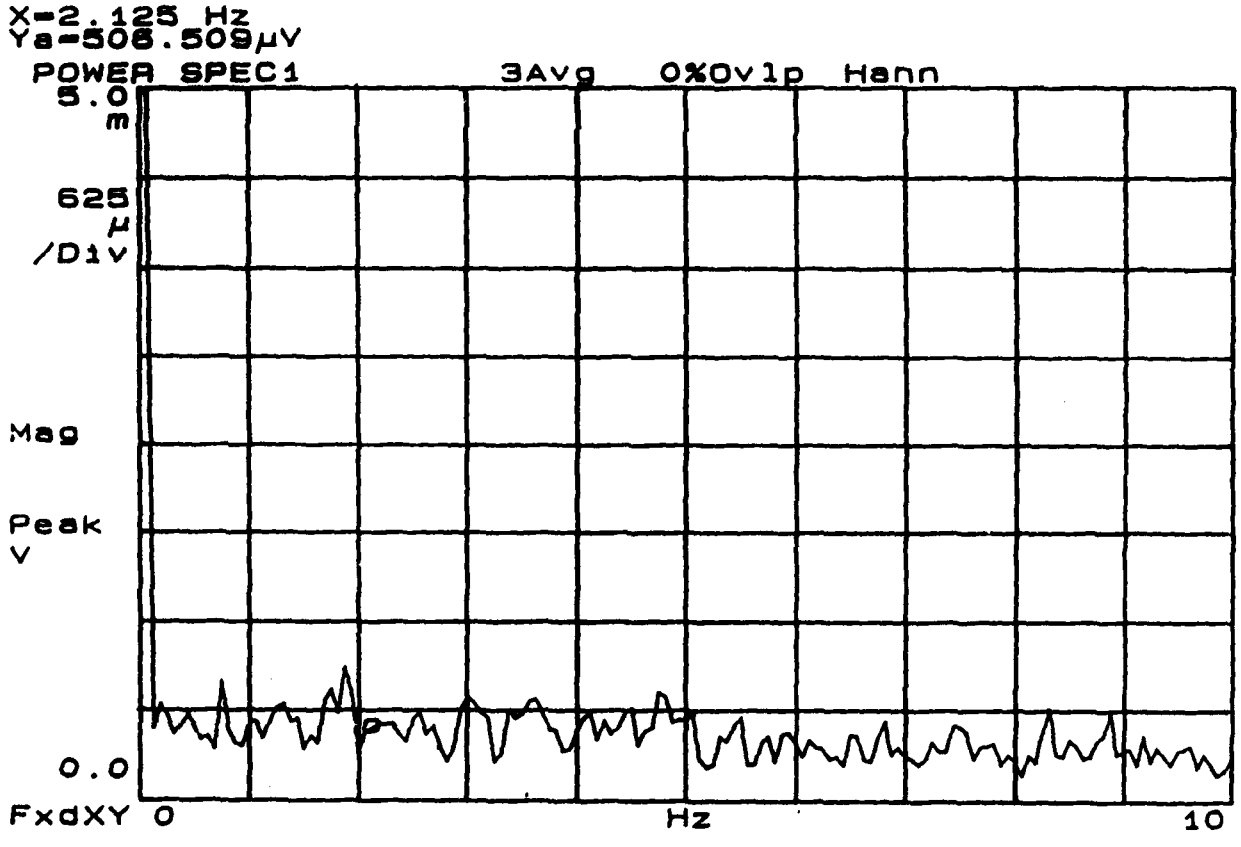

Figure 12 The noise level, which was obtained by setting the temperature modulation to zero.

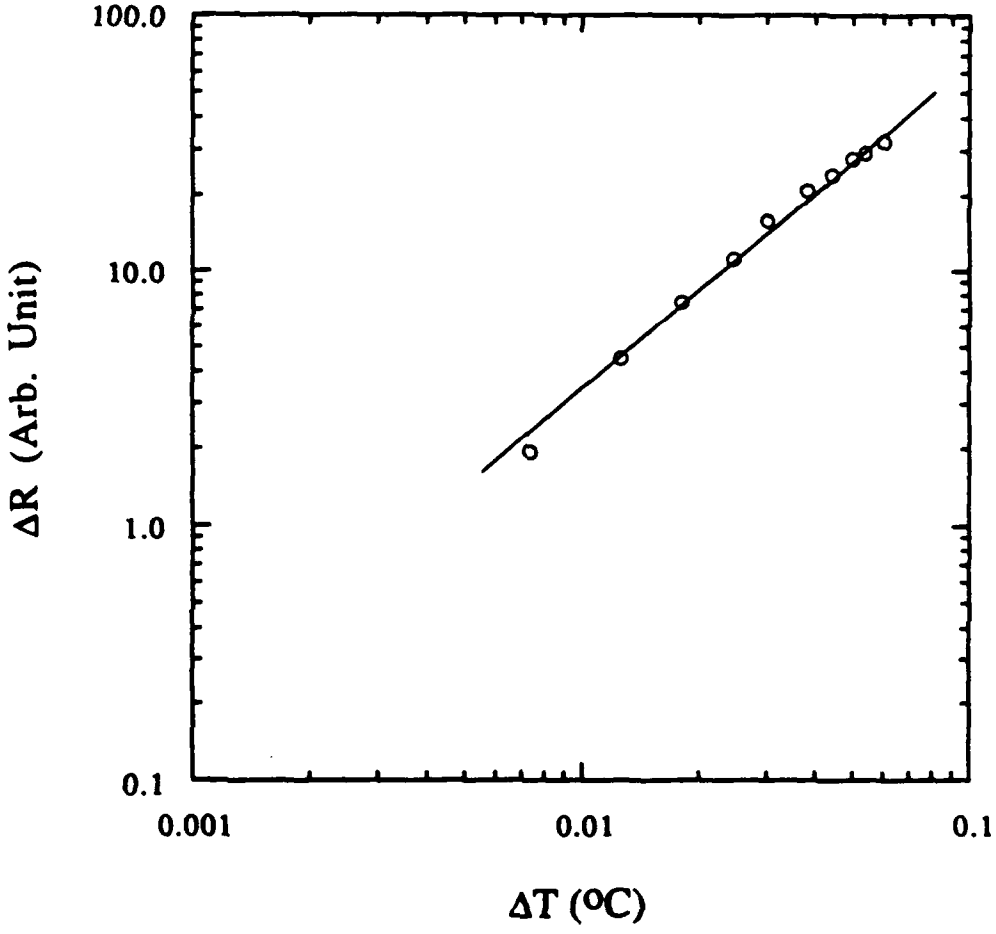

Figure 13 The dependence of the 600 nm reflectance coefficient of SbSI thin film on micro-glass at 19°C on the magnitude of the temperature modulation.

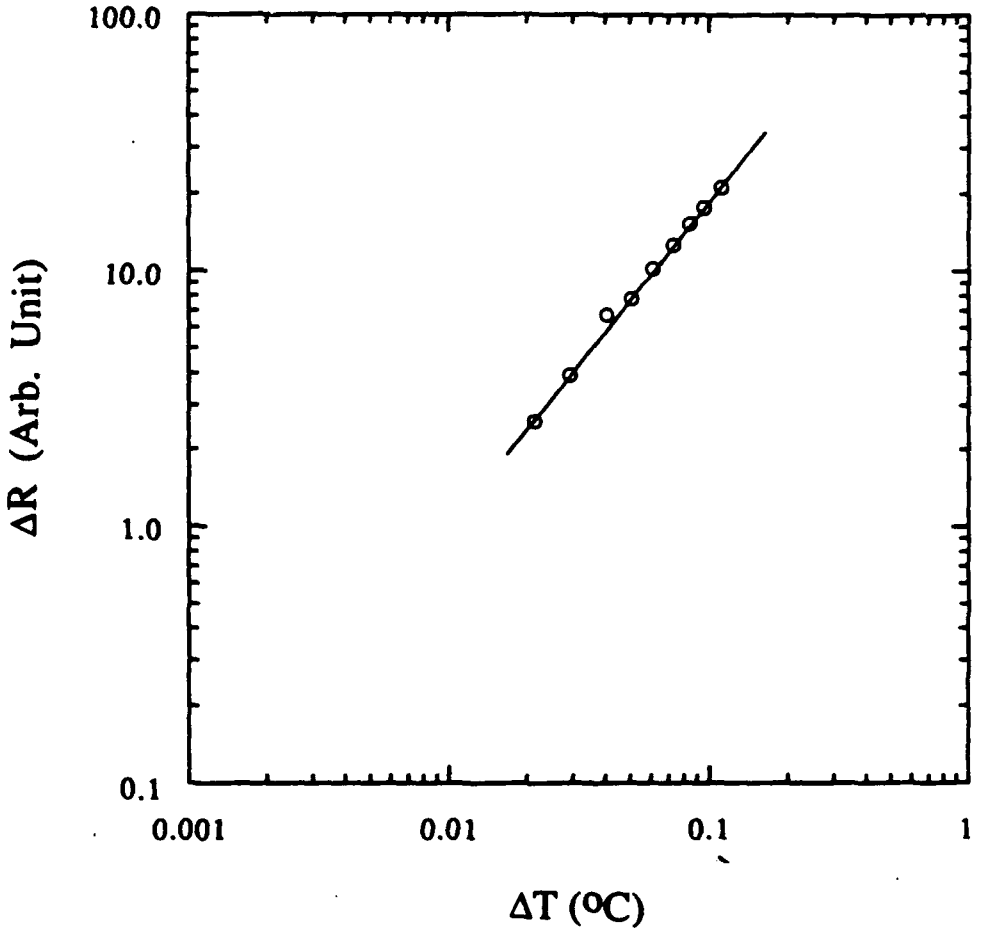

Figure 14 The change of the reflectivity with temperature modulation for a SbSI thin film on a GaAs substrate.

Table 2 Summary of the experimental results, for single crystal and thin films.

Material	λ(nm)	$\frac{\Delta<n>}{\Delta T}$ (°C^{-1})	ΔT_{min}(°C)	Temperature Range (°C)
SbSI	633	7×10^{-2}	10^{-3}	15 to 19
SbSI (on GaAs)	600	3.3×10^{-3}	2.1×10^{-2}	16 to 20
SbSI (on glass)	600	10^{-2}		16 to 20
SbSI (on thin glass)	600		0.7×10^{-2}	~16
SbSI	600		1.1×10^{-2}	~16